Mutation of two central pair apparatus genes results in severe primary ciliary dyskinesia in mice

Casey McKenzie[1] and Lance Lee[1,2]

[1]Pediatrics and Rare Diseases Group, Sanford Research, Sioux Falls, SD; [2]Department of Pediatrics, Sanford School of Medicine of the University of South Dakota, Sioux Falls, SD

Defects in motile cilia and flagella commonly result in the pediatric syndrome primary ciliary dyskinesia (PCD), a genetic and phenotypically heterogeneous disorder[1,2]. Affected individuals typically suffer from chronic rhinosinusitis, male infertility, and laterality defects, with some patients and models exhibiting female infertility and hydrocephalus. Motile cilia play a critical role in fluid flow, especially in the respiratory tract, while the structurally related sperm flagella are required for sperm motility. We previously showed that mice lacking central pair apparatus (CPA) proteins SPEF2, CFAP221, and CFAP54 each have a PCD phenotype resulting from a defect in ciliary motility[3,4,5], with *SPEF2* and *CFAP221* also known human PCD genes[6,7]. Here, we have investigated how loss of multiple CPA genes affects ciliary function and PCD pathogenesis. Each combination of double heterozygous and double homozygous mutants was generated by crossing the individual mouse lines with mutations in *CFAP221 (nm1054)*, *CFAP54 (Cfap54$^{gt/gt}$)*, and *SPEF2 (bgh)*.

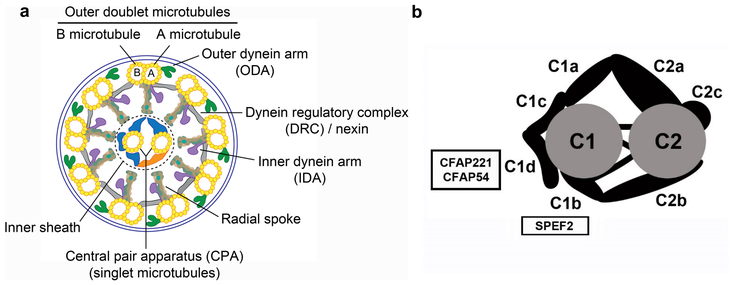

Figure 1. The ciliary axoneme. (a) Schematic diagram showing the 9+2 microtubule structure of the ciliary axoneme. From Lee and Ostrowski, 2021[2]. (b) Schematic diagram showing the basic structure of the CPA and the protein projections containing CFAP221, CFAP54, and SPEF2. From McKenzie and Lee, 2020[8].

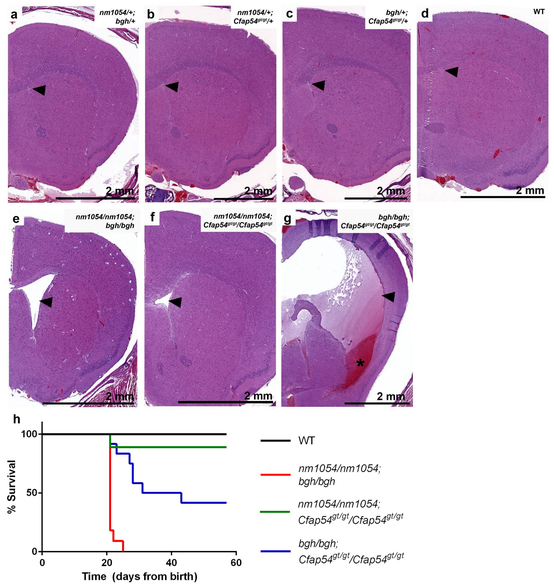

Figure 2. Severe hydrocephalus and early lethality in double mutant mice. (a-d) Coronal sections show no detectable hydrocephalus phenotype in any double heterozygous line or wild type (WT) mice. (e-g) Each double homozygous line shows ventricular dilatation (arrowhead), sometimes accompanied by intraventricular hemorrhaging. Sections stained with H&E. Hydrocephalus was only seen in single mutant lines on the susceptible C57BL6/J background[3,4,5,9], but the severe hydrocephalus is observed in all double homozygous mutants on a typically non-susceptible mixed C57BL6/J x 129S6/SvEvTac background. (h) All three double homozygous lines exhibit early lethality on a mixed genetic background, which is not seen for single mutant lines[3,4,5]. From McKenzie and Lee, 2020[8].

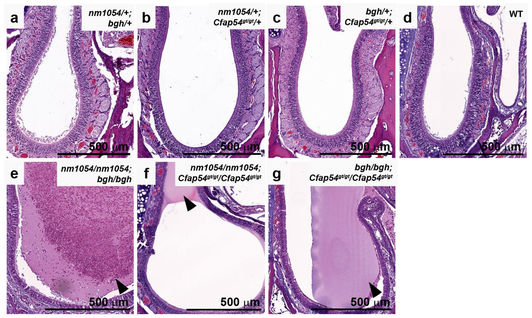

Figure 3. Sinus abnormalities in double mutant mice. (a-d) Coronal sections through the maxillary sinus cavity show no detectable airway phenotypes in any double heterozygous line or wild type (WT) mice. (e-g) Each double homozygous line shows a defect in mucociliary clearance indicated by accumulation of mucus (arrowhead) in the maxillary sinus cavity that is sometimes accompanied by infiltration of neutrophils. Sections stained with H&E. From McKenzie and Lee, 2020[8].

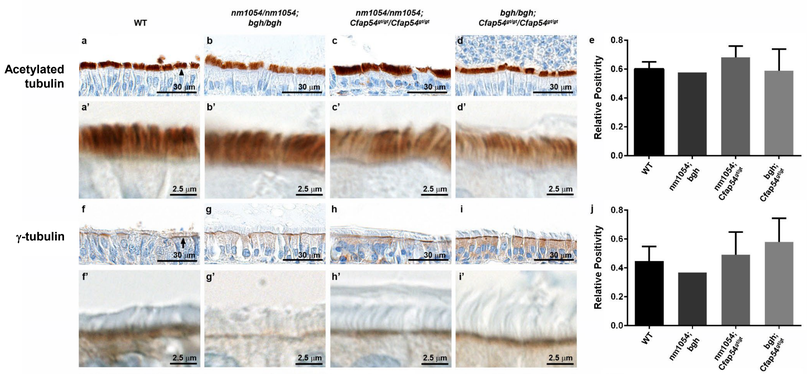

Figure 4. Normal ciliary morphology and distribution in the sinus cavity of double mutant mice. (a-d) Immunohistochemical analysis of ciliary marker acetylated tubulin (arrowhead) shows a normal appearance of motile cilia on sinus epithelial cells from WT and double homozygous mice. (e) Quantification of acetylated tubulin staining intensity showing no statistical significance as determined by one-way ANOVA. Since only one *nm1054/nm1054;bgh/bgh* mouse survived for tissue collection, no statistical analysis was performed. (f-i) Immunohistochemical analysis of basal body marker γ-tubulin (arrow) shows a normal appearance of the basal bodies. (j) Quantification of γ-tubulin staining intensity showing no statistical significance as determined by one-way ANOVA. The apparently normal staining patterns for ciliary and basal body markers indicate that there are no substantial defects in ciliogenesis in double homozygous mice. From McKenzie and Lee, 2020[8].

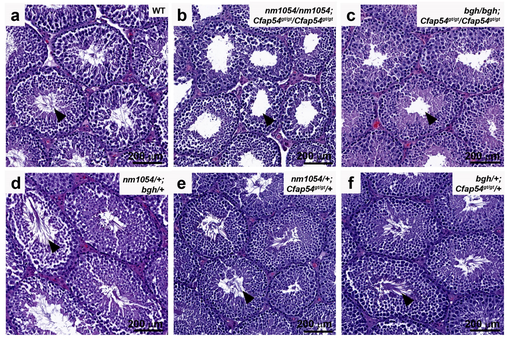

Figure 5. Spermatogenesis defects in double mutant mice. Testis histology shows an absence of flagellar formation in the lumen of the seminiferous tubule (arrowhead) from each double homozygous mouse line (b,c) compared to WT (a) or double heterozygotes (d-f), indicating that spermatogenesis is aborted. No male *nm1054/nm1054;bgh/bgh* mice survived for tissue collection. Sections stained with H&E. From McKenzie and Lee, 2020[8].

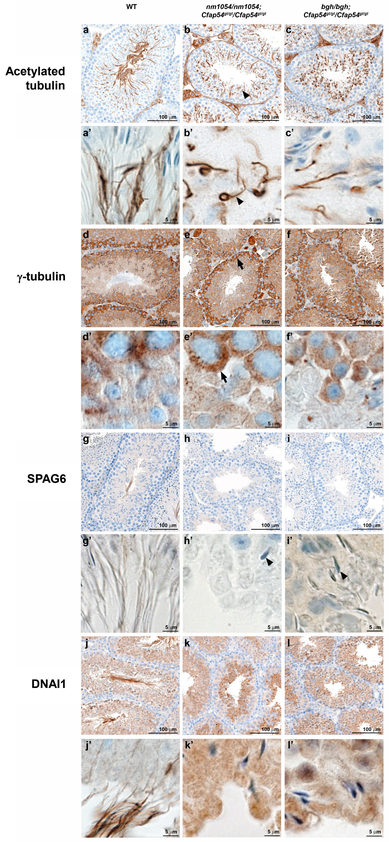

Figure 6. Sperm flagellar formation defects in the double mutant testis. (a-c) Immunohistochemical analysis of flagellar marker acetylated tubulin shows rudimentary axonemal structures being formed in the double mutant testis (arrowhead). (d-f) Normal staining for basal body marker γ-tubulin in the immature spermatogonia and developing spermatocytes of the double mutant testis (arrow) suggests that early spermatogenesis stages are unaffected. (g-i) CPA protein SPAG6, which is detected in the WT flagellar axoneme, shows no clear staining pattern in double mutants. The axonemal structures detected by the acetylated tubulin antibody are not detected by the SPAG6 antibody, indicating that that CPA assembly may be perturbed. Only occasional sperm heads are observed (arrowheads). (j-l) In contrast to SPAG6, dynein marker DNAI1 shows strong expression in the developing spermatids of double mutant mice, suggesting that dynein pre-assembly may occur in the spermatid cytoplasm before spermatogenesis is aborted. No male *nm1054/nm1054;bgh/bgh* mice survived for tissue collection. From McKenzie and Lee, 2020[8].

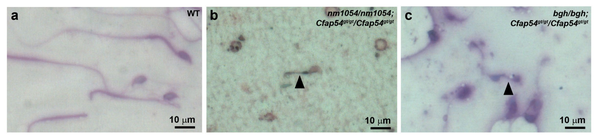

Figure 7. Abnormal epididymal sperm in double mutant mice. WT epididymal sperm are abundant and have a normal morphology (a), while mature sperm are rare in the epididymis of double homozygous mice (b,c). When present, double mutant sperm have severely shortened flagella (arrowhead). Cells stained with the Camco differential stain kit. From McKenzie and Lee, 2020[8].

Severe phenotypes in double homozygous mice indicate genetic interactions between CPA genes and demonstrate the importance of the CPA in regulating proper ciliary function. Further, the severity of the spermatogenic defects compared to the morphology of motile cilia underscores fundamental mechanistic differences between ciliary and flagellar biogenesis.

Acknowledgments: We gratefully thank Claire Evans, Carol Dao, and Matthew Billion for technical assistance. This work was funded by Sanford Research. The Sanford Research Histology & Imaging Core was supported by NIH grant P20GM103548, and Carol Dao was supported by NIH grant R25HD097633.

References:

1. Wallmeier et al., 2020. *Nat. Rev. Dis. Primers.* 6:77.
2. Lee and Ostrowski, 2021. *Cell. Mol. Life Sci.*, 78: 769-797.
3. Lee et al., 2008. *Mol. Cell. Biol.* 28: 949-957.
4. Sironen et al., 2011. *Biol. Reprod.* 85: 690-701.
5. McKenzie et al., 2015. *Mol. Biol. Cell* 26: 3140-3149.
6. Cindric et al., 2020. *Am. J. Respir. Cell Mol. Biol.* 62: 382-396.
7. Bustamante-Marin et al., 2020. *J. Hum. Genet.* 65: 175-180.
8. McKenzie and Lee, 2020. *Sci. Rep.* 10: 12337.
9. Finn et al., 2014. *Neurosci.* 277: 552-567.